JOURNAL OF VIROLOGY, Oct. 1976, p. 264-272
Vol. 20, No. 1

Printed in U.S.A.

Size, Subunit Composition, and Secondary Structure of the Friend Virus Genome[1]

SHYAM DUBE, HSING-JIEN KUNG, WELCOME BENDER, NORMAN DAVIDSON,* AND WOLFRAM OSTERTAG

Department of Chemistry and Division of Biology, California Institute of Technology, Pasadena, California 91125, and Max Planck Institut für Experimentelle Medizin, Göttingen, Germany*

Received for publication 5 May 1976

Electron microscope and gel electrophoresis studies show that the high-molecular-weight (50 to 70S) RNA extracted from Friend virus (FV) is a dimer with the same basic structure previously observed for the RNAs from RD-114 virus, baboon virus, and woolly monkey virus. This observation greatly strengthens the inference that the dimer structure is a general characteristic of the RNAs of all mammalian type C viruses. The FV dimer is slightly less stable than the RNA dimer of woolly monkey virus, which is, in turn, much less stable than those of RD-114 and baboon virus. There are three FV monomer components, small (S), medium (M), and large (L), with molecular lengths of 6.7 ± 0.6, 7.7 ± 0.6, and 9.5 ± 0.6 kilobases, respectively. There are approximately equal amounts of the S and M components and much less of the L component. Most of the dimers are homodimers (SS, MM, and LL). The frequency of heterodimers (SM, SL, ML) is much less than expected for a random assortment model.

Friend virus (FV) (7) preparations are known to contain two viral components with different biological activities (1, 10, 16), the spleen focus-forming virus, and the lymphatic leukemia virus. The spleen focus-forming virus is oncogenic; it transforms erythroid precursor cells and induces spleen focus formation, thus resulting in erythroleukemia in mice. The spleen focus-forming virus is replication defective and needs a helper virus. The helper function is provided by the lymphatic leukemia virus component of the FV complex (16). The helper function can be provided by many other murine leukemia viruses (for example, Moloney leukemia virus), which do not induce erythroid disease (16). The endogenous virus released during dimethyl sulfoxide-induced differentiation of Friend cells (5) and upon exposure of these cells to bromodeoxyuridine also has helper activity (5, 14).

Earlier work on the FV genomic RNA has shown that: (i) the FV RNA contains two subunits whose sedimentation coefficients are approximately 35 and 32S; (ii) the amount of the larger subunit is ≤20%, whereas the smaller subunit constitutes 80% or more of the FV RNA; (iii) the genomic complexity is approximately 2.5×10^6 daltons; and (iv) the viral RNA contains polyadenylic acid [poly(A)] and also internal oligo(A) tracks (12). In addition, the 35 and 32S subunits have been tentatively assigned to lymphatic leukemia virus and spleen focus-forming virus RNA, respectively (11).

Electron microscope studies from this laboratory have shown that the high-molecular-weight (50 to 70S typically) RNA components extracted from several different type C viruses all have a common structure (3, 8, 9). They are dimers consisting of two monomers with molecular weights of about 3×10^6, joined together at their 5′ ends by a secondary feature called the dimer linkage structure (DLS). There is a loop close to the middle of each monomer, and there is a poly(A) stretch at each 3′ end. This structure has been observed for RD-114, an endogenous xenotropic cat virus; for BKD, an endogenous xenotropic baboon virus; and for WoMV, a virus horizontally transmitted in woolly monkeys. It was of interest, therefore, to ask whether a murine type C virus has the same structure. The Friend system is of additional interest because it contains both transforming and leukemogenic activities and because Friend cells are a system in which to study the relation between expression of viral and cellular genes.

MATERIALS AND METHODS

Stock solutions. NTE buffer consisted of 0.1 M NaCl, 0.01 M Tris-OH, and 0.001 M EDTA, adjusted to pH 7.5 with HCl.

(U+F) solvent. A 480-g quantity of urea was dissolved in 1 liter of formamide, giving 1.35 liters of

[1] Contribution no. 5302 from the Department of Chemistry, California Institute of Technology, Pasadena, CA 91125.

solution. The volume percentage of this solution when mixed with aqueous electrolyte is reported as percent (U+F). (See reference 8 for explanation.)

E buffer. E buffer consisted of 0.05 M boric acid, 0.005 M sodium borate ($Na_2B_4O_6 \cdot 10H_2O$), 0.01 M Na_2SO_4, and 0.001 M EDTA (pH 8.2).

TE buffer. A y molar concentration of TE buffer contains (per liter) y moles of Tris OH and 0.1 y mol of Na EDTA, all adjusted to pH 8.5 with HCl. The cation concentration is 0.3 y in Na^+ ions, approximately 0.3 y in Tris H^+, and therefore contains 0.6 y total.

Cells, virus, and RNA. The cell line used, FSD-3, has been described previously (4). Briefly it originated as follows. FV containing cell-free supernatant from a cell culture of an FV-transformed cell line, FSD-1 (13), clone F_4, was injected intraperitoneally into BALB/c mice. Spleen cells from these mice were used to start the FSD-3 cell line. FV was isolated from these cells as described (5). FV twice purified by isopycnic banding in a 24 to 48% sucrose gradient was used for RNA isolation. The viral pellet was suspended in 1% sodium dodecyl sulfate, and to this an equal volume of a mixture of phenol, chloroform, and isoamyl alcohol (50:2:48) was added. Viral RNA was precipitated from the aqueous phase by ethanol and purified by sedimentation on a 10 to 30% NTE-sucrose gradient for 75 min at 4°C in a Beckman SW50.1 rotor. Fractions were collected and monitored for absorbance at 260 nm. The peak fractions in the 50 to 60S region were pooled, precipitated with ethanol, and used for the present studies.

Agarose gel electrophoresis. All gel electrophoresis experiments were conducted on 1% agarose gels in E buffer. The preparation of the non-denaturing gels and of the strongly denaturing CH_3HgOH gels has been described (2, 8). In the experiments for studying the dissociation temperature of the 50 to 60S RNA, RNA samples were mixed with (U+F) solvent and NTE buffer to the desired concentrations. Samples (ca. 20 μl) were sealed in a capillary tube, incubated for 5 min at the desired temperature, mixed with glycerol and bromophenol blue, and loaded onto the gels. Electrophoresis was performed at 5 mA/tube for 3 h at room temperature. The gels were then stained with 1 μg of ethidium bromide per ml in 0.5 M NH_4Ac for 30 min and examined by illumination with short-wavelength UV light.

For agarose gel electrophoresis experiments using CH_3HgOH as a denaturing agent, RNA samples were mixed with CH_3HgOH in E buffer to a final concentration of 5 mM CH_3HgOH and loaded onto a 1% agarose gel containing 5 mM CH_3HgOH. Electrophoresis was performed for 4 h at 25°C at 5 mA/tube.

Electron microscopy. The urea-formamide and the glyoxal-formamide spreading techniques have been described previously (3, 8, 9). In the urea-formamide spreading, RNA samples were diluted into the spreading solution which contained about 30 μg of cytochrome *c* per ml and the desired concentration of (U+F) and electrolyte. The hypophase was double-distilled water. To study the structure of undissociated 50 to 60S RNA, the spreading was performed in 80% (U+F) solution containing 0.15 M TE ($\approx$0.09 M cations in the final solution). These conditions cause only partial melting of the 50 to 60S RNA. In the experiments to determine the molecular weights of dissociated subunits, RNA samples were first treated with 85 to 90% (U+F) in $\leq$0.05 M TE, and were then either spread directly from 85% (U+F) or diluted and spread from 60% (U+F). Essentially identical results have been obtained from these spreadings.

Our standard glyoxal-formamide technique involves treatment of the RNA with 1 M glyoxal and 0.01 M phosphate buffer, pH 6.7, at 37°C for 1 h. A less-denaturing treatment is with 1 M glyoxal, 0.01 M phosphate buffer, and 0.05 M NaCl at 37°C for 1 h. The glyoxalated RNA is then either diluted 10-fold or more into spreading solution of 30% formamide and 0.1 M TE or dialyzed into this solution and spread onto 5% formamide and 0.01 M TE.

The technique for mapping of poly(A) segments on RNA molecules using simian virus 40 (SV40) circles with polydeoxythymidylate [poly(dT)] tails has been described previously (3). Conditions of electron microscopy are as previously described. Magnifications were measured with a diffraction grating and/or using circular SV40 as an internal standard.

RESULTS

RNA components of FV complex from FSD-3 cells. In non-denaturing (i.e., high salt, NTE) sucrose gradients, FV RNA sedimented as a single peak with a sedimentation coefficient of 50 to 60S. When this RNA fraction was collected and subjected to electrophoresis in non-denaturing agarose gels, a single diffuse band (Fig. 1b) with an apparent molecular weight of 5×10^6 to 6×10^6 was reproducibly observed. If, however, the RNA samples were first treated with a denaturing solvent [i.e., dissolved in 66% (U+F), 0.03 M cations] at 25°C and then applied onto the agarose gel, about 50% of the FV RNA dissociated into subunits. This was evidenced by the appearance of three faster-moving bands in addition to the original diffuse band. Upon heating to 40°C in the same solvent [66% (U+F), 0.03 M cations] the diffuse band dissociated completely; there were only the three faster bands plus a broad distribution of lower-molecular-weight fragments. (This gel pattern is not illustrated, but a similar pattern obtained in methyl mercury gels is described below.) Treatment of RNA with more denaturing conditions [90% (U+F), 0.03 M cations] at 40°C did not cause further dissociation.

The three-band pattern has been observed for the heat-dissociated FV RNA extracted from several different virus preparations. The two bands with higher mobility, referred to as S (for small) and M (for medium), had comparable fluorescent intensities when stained with ethidium bromide; L (large), the slowest moving band, had about one-third the intensity of the S or M bands.

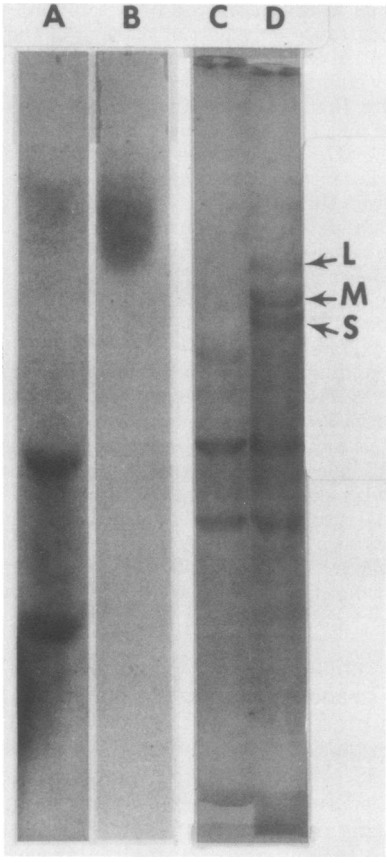

FIG. 1. *Electrophoretic gel patterns in 1% agarose. (A) and (B) are nondenaturing gels run in parallel; (C) and (D) are denaturing gels containing 5 mM CH_3HgOH run in parallel. (A) HeLa 28 and 18S ribosomal RNA. (B) 50 to 60S FV RNA. (C) HeLa 28 and 18S rRNA and Escherichia coli 23S ribosomal RNA. (D) same as (C) plus 50 to 60S FV RNA. L, M, and S denote the large, medium, and small subunits of FV RNA.*

Molecular weight estimates by gel electrophoresis. CH_3HgOH (5 mM) is a strong denaturant for nucleic acids and agarose gel electrophoresis. CH_3HgOH is useful for measuring molecular weights of RNA polynucleotide strands with minimal effects due to secondary structure (2). An experiment on FV RNA is shown in Fig. 1D; again three discrete bands are observed, with the slow (L) component being the faintest.

A plot of log (molecular weight) versus mobility for the molecular weight standards in Fig. 1C and 1D and for the three FV components, S, M, and L, is shown in Fig. 2. A rough visual estimate of the band widths of the three components is also shown in the figure. This plot leads to molecular weight estimates of $2.33 \times 10^6 \pm 0.2 \times 10^6$, $2.65 \times 10^6 \pm 0.2 \times 10^6$, and $3.27 \times 10^6 \pm 0.2 \times 10^6$, corresponding to kilobase (kb) lengths of 6.7 ± 0.6, 7.7 ± 0.6, and 9.5 ± 0.6, for the S, M, and L components, respectively.

Electron microscope studies. To extend the molecules into filaments with a recognizable topology and reproducible length for electron microscopy, RNA must be spread from partially denaturing solvents. The dimer structures of RD-114 and BKD RNAs are quite stable and easy to preserve under suitable spreading conditions (8, 9). WoMV RNA dimers dissociate more readily, and it is necessary to delicately adjust the spreading conditions to observe the dimer structure (9). We observe that FV RNA has a dimer structure which is slightly less stable towards dissociation than is WoMV RNA.

The two partial denaturation techniques that we have found to be particularly useful for electron microscopy involve: (i) treatment with and spreading from a (U+F) solvent and (ii) treatment with glyoxal followed by spreading from a rather low-percent formamide solvent, usually 40%. The urea-formamide method permits quantitative control of denaturing conditions. The glyoxal method is used when it is desired to identify the poly(A) ends of the RNA molecules by hybridization to circular duplex SV40 DNA with attached poly(dT) tails (3). As explained below, a sample of molecules with labeled poly(A) ends is particularly useful for reliable length measurements on molecules known to be unbroken.

When FV RNA is treated with 90% (U+F),

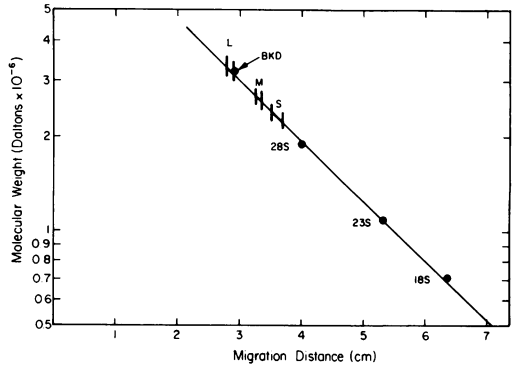

FIG. 2. *A plot of RNA electrophoretic mobility versus molecular weight for the CH_3HgOH gel shown in Fig. 1D. Symbols: (●) Indicates the position of a molecular weight standard; (⊢⊣) indicates the band width of FV RNA. The baboon viral RNA (BKD) marker was labeled with ^3H, and its position was determined by slicing the gel into 1-mm disks and counting.*

0.03 M cations, and then spread from 60% (U+F), 0.03 M cations, polynucleotide strands with a broad distribution of molecular lengths ranging from 0 to about 2.0 μm and with no discernible secondary structure are seen. Some typical examples are shown in Fig. 3a. A histogram of the length distribution shows a peak in the range of 1.7 to 1.9 μm, corresponding to molecular lengths in the range of 6.7 to 7.5 kb. As shown below these are monomer units of FV RNA.

When FV RNA is spread from 80% (U+F), 0.09 M cations, about 70% of the molecules are sufficiently extended to be traceable. Many of these molecules, such as the one shown in Fig. 3c, have about twice the length of the filaments shown in Fig. 3a and are, therefore, dimers. They have the same basic structure seen previously for the dimers of RD-114, BKD, and WoMV RNAs. There is a central DLS, which in this case is rather small, and sometimes, as in Fig. 3c, there is a secondary structure loop in the middle of a monomer. In the case of FV RNA, there are often several crossover points

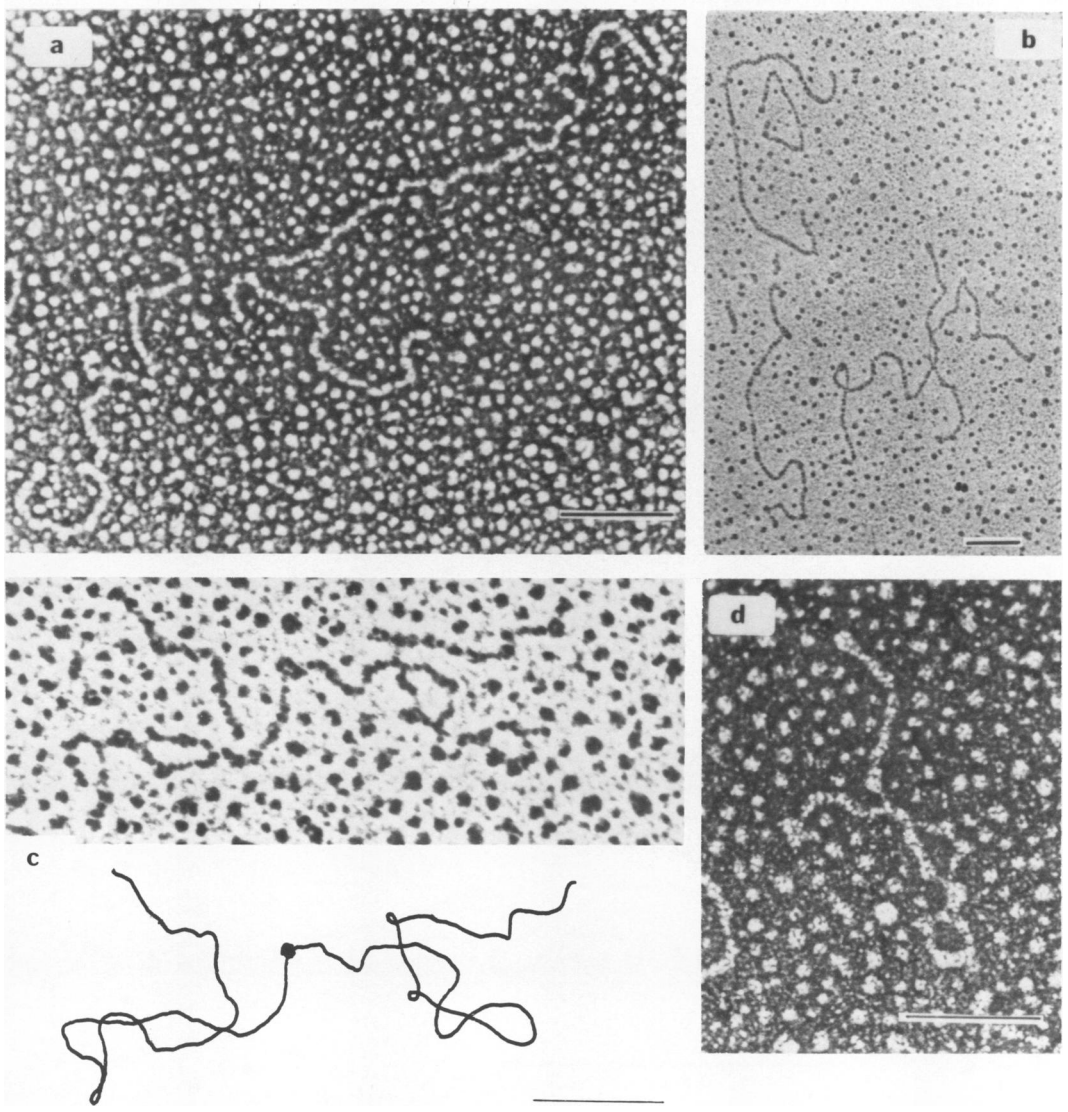

FIG. 3. *Electron micrographs of FV RNAs. (a) A 90% concentration of (U + F) solvent (0.03 M cations) treated and spread from 60% (U + F). (b) Glyoxal treated and spread from 30% formamide (0.06 M cations). (c) and (d) A 80% (U + F) solvent (0.09 M cations) treated and spread in the same medium. An interpretive tracing of the molecule in (c) is shown. All spreading procedures are described in Materials and Methods. The length marker is 0.2 μm.*

within the loops. In the same spreading some monomers are seen, and some of these still have the secondary structure loop (Fig. 3d). Under the spreading conditions used, about 50% of the traceable molecules are of monomer length or shorter.

If FV RNA is incubated with 1 M glyoxal in 0.01 M phosphate buffer at 37°C for 1 h, and the resulting RNA is spread from 30 or 40% formamide, 0.06 M cations, there are a few dimers, but most of the RNA molecules are smooth structureless filaments with molecular lengths of up to 1.9 μm. Thus, this treatment causes considerable dissociation of the FV RNA into monomers. However, if the RNA is treated with glyoxal at a higher salt concentration and spread from 40% formamide, 0.06 M cations, many more dimer molecules are seen. Poly(A) tails on RNA molecules treated with glyoxal can be mapped in the electron microscope by hybridizing to circular SV40 containing poly(dT) tails (3). Examples of such molecules are shown in Fig. 4. They contain a central DLS, loops close to the middle of each monomer component, and poly(A) ends attached to SV40-(dT). There are some incomplete dimers consisting of a complete monomer joined to a broken monomer. These have a recognizable DLS,

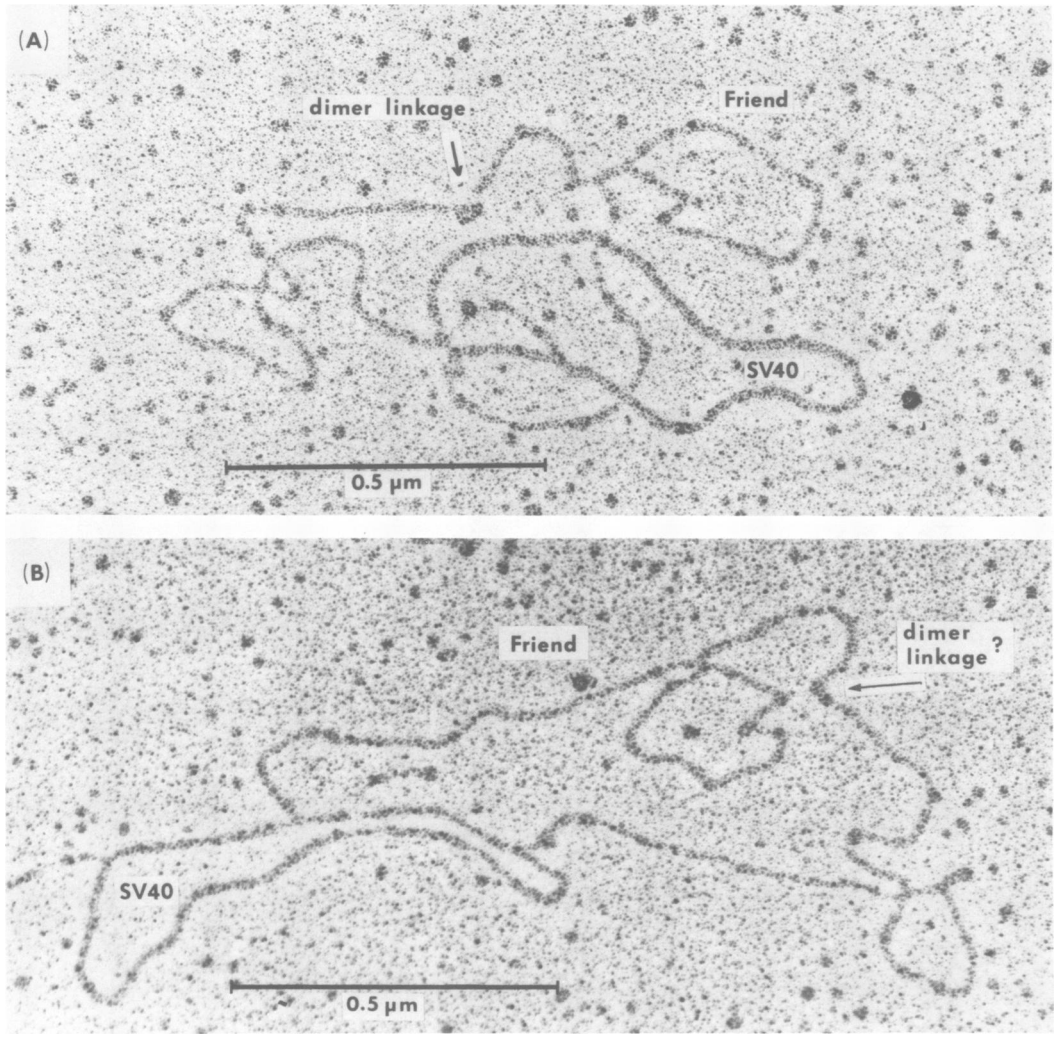

FIG. 4. *Poly(A) mapping on FV dimers. The poly(A) sequences at both outside ends of an FV 50 to 60S RNA dimer anneal to short poly(dT) sequences polymerized onto SV40 circles. Both dimers show the characteristic loops on each monomer half. The DLS in (B) is indistinct, as is true for many FV dimers. All subunits here are of medium size (7 to 8 kb).*

with one long strand with an end attached to SV40(dT), and with one short strand with no SV40(dT). The monomer constituent here and the two monomer constituents of a complete dimer with two attached SV40(dT)'s can be used with confidence for length measurements of full-length monomers. Figure 5 shows a histogram of the length distribution for all complete monomers, either from unbroken dimers or from dimers with one intact monomer unit. As explained in the legend to Fig. 5, the length calibration is based on measurements with BKD viral RNA treated with glyoxal and spread under the same conditions as used for FV RNA.

The distribution in Fig. 5 shows two partially resolved main components with an average molecular length of 6.2 ± 0.2 kb for the smaller (S) component and 7.4 ± 0.5 kb for the medium (M) component. These values are in reasonable agreement with the molecular weights of 6.7 ± 0.6 and 7.7 ± 0.6 kb for the S and M components measured by gel electrophoresis under denaturing conditions.

There are a few monomer units with molecular lengths in the broad range from 8.5 to 10.5 kb in Fig. 5. This range more or less agrees with the molecular length of the large (L) component in the gel electrophoresis experiment of 9.5 ± 0.6 kb. However, the molecules in the fraction labeled L in Fig. 5 have a peculiar skewed distribution. In view of the small sample of molecules, we cannot draw conclusions as to whether there is one or several size classes in this L component or whether the electron microscope and gel electrophoresis data are really in good agreement.

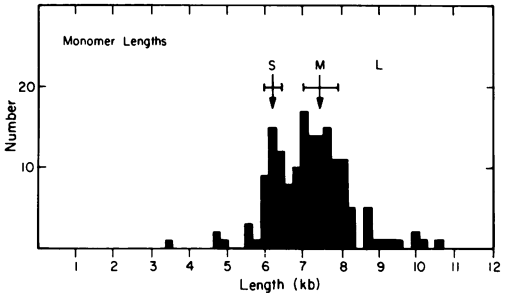

FIG. 5. *Distribution of monomer subunit lengths. All unbroken monomers that had their 3' poly(A) ends attached to SV40-poly(dT) and their 5' ends in a clearly recognizable DLS were measured, and their total contour lengths were plotted. Regions of the histogram are designated S, M, and L, corresponding to the small, medium, and large subunits seen on denaturing gels. The average sizes (arrow) and standard deviations (brackets) are indicated for the small (6.2 ± 0.2 kb) and medium subunit regions (7.4 ± 0.5 kb). For length calibration, E. coli 23S ribosomal RNA, treated by the standard glyoxal procedure, was spread and measured. The FV RNA for this figure was glyoxal treated in the presence of 50 mM NaCl. BKD viral RNA, after treatment with glyoxal in this salt medium, measured 4.4% shorter than after the standard glyoxal treatment, and this correction factor was included. This leads to the calibration that 1 μm = 4.1 kb.*

Given that there are S, M, and L monomer units, we may ask whether the dimers found are all homodimers SS, MM, or LL or whether the heterodimers, SM, SL, and ML are also present. To study this question, we plot in Fig. 6 the length of the long arm of each dimer versus the length of the short arm. Due solely to statistical fluctuations, the measured lengths of the two monomer arms of any one homodimer will, in general, be different. The nature of the plot in Fig. 6 is such that all points must lie below the straight line of slope 1.00 indicated on the figure. The figure also has a dotted line with a slope of 0.89 going through the origin. The usual standard deviation in length for a homogeneous RNA component is about 8%. As explained in the figure legend, if only homodimers are present, we would expect most of the points to lie within a vertical distance of about 1.4 standard deviations in length for a homogeneous component below the slope 1.00 line, that is, within the sector between the lines of slope 1.00 and 0.89.

Suppose the relative frequencies of the S, M, and L components are s, m, and l. Suppose dimers are formed by random association. Then the relative numbers of the several components would be s^2, m^2, l^2, 2 sm, 2 sl, and 2 ml. The random association model would predict that there would be a considerable density of points below the sector defined by the two straight lines of slopes 1.0 and 0.89. However, there are relatively few such points in Fig. 6.

To give a specific example, suppose there were the number of SM heterodimers expected for random assortment. There are about 30 points in Fig. 6 in the x interval of 6 to 7 kb within the two lines and about 30 points in the x interval of 7 to 8 kb. Then there should be about 60 points clustered in a Gaussian distribution around the coordinates x = 7.4 kb, y = 6.2 kb. Similarly, there are perhaps 6 LL dimers in Fig. 6. For random assortment, there ought to be about 27 SL and 27 ML dimers clustered around the points x = 9.5 kb, y = 6.2 kb and x = 9.5 kb, y = 7.4 kb. These three expected heterodimer positions are marked in the figure. It is clear that in no case is there this predicted frequency of heterodimers. In fact,

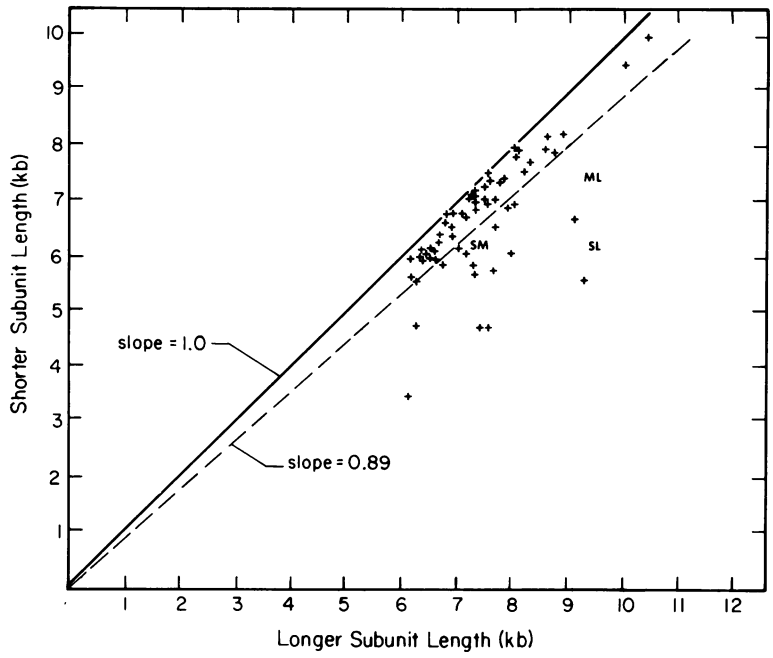

FIG. 6. *Correlation of the two monomer lengths in dimer molecules. All complete dimer RNA molecules with both poly(A) monomer ends joined to SV40-poly(dT) and with clear DLS were measured and plotted. Each cross represents one dimer molecule; its x and y coordinates are the contour lengths of the longer and shorter subunits of the dimer, respectively. It can be shown that, if dimers consists of subunits of identical length and if the standard deviation for the subunit lengths is σ, the distribution curve of the difference (x − y) is: f[(x − y)] = A exp [−(x − y)²/4σ²]. Thus, the standard deviation (σ') of the difference distribution curve is (2σ²)^1/2 = 1.4 σ. The standard deviation in length for tumor virus RNAs containing only a single monomer component is about 8% (9). If both halves of Friend dimers are always identical, and if the only length difference is due to measurement error, 68% of the dimers should have monomers differing by less than 1.4 × 8% = 11%, and these molecules will be plotted above the line with a slope of 0.89. If heterodimers are formed, they should be found centered at the positions marked SM, SL, and ML.*

the number of points below the 0.89 line is approximately the number expected due to statistical variations in length, assuming no heterodimers. Furthermore, a few of the outside points may be artifacts due, for example, to a broken monomer strand accidentally lying on an SV40 label. We can positively conclude that the frequency of heterodimers is much less than expected for random assortment of monomers, but we cannot decide whether heterodimers are completely absent or are present at a low, but nonzero, frequency.

Figure 7 and its legend summarize the appearance and length data for the several secondary structure features found in FV RNA. The DLS is often hard to identify; at best it looks as shown in Fig. 7d; at worst it is not discernible at all. The loops frequently have multiple crossover points (Fig. 7b and c), suggesting that there are multiple junctions therein. The histograms of loop length and of distance from the 5′ end or from the 3′ end (not shown) are broader than observed for RD-114, BKD, and WoMV, perhaps because different members of the multiple junction points are open or closed for different molecules. If there are multiple-loop junctions, some of which are open and some of which are closed in any one molecule, then the position of the center of the loop relative to an end of the molecule should be more constant than the loop length. This is indeed the case. The average distance from poly(A) end to the center of the loop for the several size classes of RNA are tabulated in the legend to the figure.

DISCUSSION

The first and most basic point is that RNA from the murine virus, FV, shows the same dimer structure as seen previously in BKD, RD-114, and WoMV RNAs. This observation strengthens the inference that the dimer structure is a general characteristic of the RNAs of all mammalian type C viruses.

The three general features of the dimer structure are: the DLS joining the two monomer

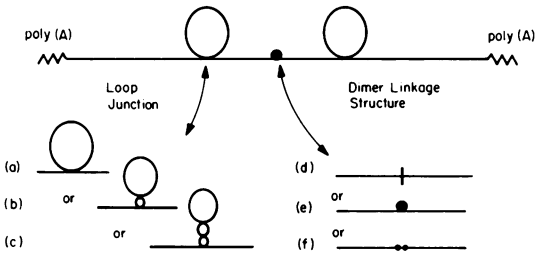

FIG. 7. *Diagram of the structure of FV RNA dimers. (a), (b), and (c) show alternate appearances of the large loop, and (d), (e), and (f) show different morphologies seen at the dimer linkage. For all monomer subunits with single loop junctions as shown in (a), the distance from poly(A) end to loop junction is 2.8 kb, the loop circumference is 2.7 kb, and the loop junction to dimer linkage distance is 1.5 kb. All these distances are about 20% longer in medium (between 6.9 and 8.4 kb) subunits than in small (between 5.9 and 6.5 kb) subunits, and the standard deviations as percentages for all these measurements are about 25%. The distance from poly(A) end to the midpoint of the loop, measured for all molecules with either single or multiple loop junctions, is 4.2 kb ± 17%. This distance for medium subunits only is 4.4 kb ± 10% and for small subunits is 3.6 kb ± 5%.*

units close to their 5′ ends, a loop feature close to the center of each monomer subunit, and a poly(A) segment at the two outside ends. Since each of these features occurs quite generally for type C viral RNAs, each has probably evolved for a biological function common to all type C viruses.

Different RNAs differ in the stability of the dimer linkage. In the case of FV, we observe that the midpoint of the transition occurs at about 25°C in 66% (U+F), 0.03 M cations. We estimate that this corresponds to a melting temperature of 60°C in aqueous 0.1 M Na^+. The corresponding melting temperatures of BKD, RD-114, and WoMV RNAs are 87, 87, and 66°C, respectively.

[The conversion of melting temperature in (U+F) solvents to that in aqueous solution with 0.1 M Na^+ is based on the following equation: ΔT_m = 0.4 × percent (U+F) + 16.6°C log ([cations]), where T_m is the melting temperature. The predicted effect of cation concentration in the above equation is taken from Schildkraut and Lifson (15) and is probably fairly accurate. The estimated effect of (U+F) concentration is based on very limited data. Friedrich and Feix (7) show that the melting temperature of the double-stranded replicative form of MS2 RNA is depressed by 0.3 to 0.5°C per percentage of formamide. The melting point depression of DNA by (U+F) and by pure formamide are approximately the same per volume percent solvent (8). If we assume the same is true for RNA duplexes, we arrive at the equation above.]

These predicted melting temperatures in aqueous 0.1 M Na^+ from the equation may not be very accurate. However, the qualitative fact that the FV dimer is much less stable than that of RD-114 and BKD RNAs and slightly less stable than WoMV dimers is quite clear.

The dimer molecule also contains two loops, symmetrically disposed with respect to the DLS. The loops are also seen in monomers spread under moderately denaturing conditions (Fig. 3). Roughly speaking, these loops are of comparable stability in RD-114, BKD, WoMV, and FV RNAs.

We observe that the RNA from viruses derived from FSD-3 cells contains three monomer size classes, L, M, and S, of approximate molecular weights of 3.3 × 10^6, 2.7 × 10^6, and 2.3 × 10^6. The M and S components are present in roughly equal amounts and represent about 80 to 90% of FV RNA. The electron microscope data on complete dimers show that either heterodimers are not present or present at a frequency much less than expected for a random assortment model.

By comparison of the RNA gel patterns of FV with those of other murine sarcoma-leukemia virus complex, Maisel et al. (11) have suggested that the M and L components may be assigned to the spleen focus-forming virus and lymphatic leukemia virus activities, respectively. The L and M subunit classes in relative amounts similar to that observed here have been consistently found in many other FV-transformed cell lines (S. Dube and W. Ostertag, private communication). The S component, however, has not been described previously. The induction of an endogenous virus in FV-transformed cells has been described (5, 14). Perhaps S RNA is from the endogenous virus. Alternatively, the S component may be a deletion mutant of the M component. Nucleotide sequence studies on resolved bands are underway to determine if the S and M components are related.

ACKNOWLEDGMENTS

S.D. has been supported as a Sherman Fairchild Distinguished Scholar at the California Institute of Technology. W.B. has been the recipient of a National Science Foundation fellowship and of a training grant from the National Institutes of Health. This research has been supported by a contract, NO-1-CP-43306 within the Virus-Cancer Program of the National Cancer Institute.

LITERATURE CITED

1. **Axelrad, A. A., and R. A. Steeves.** 1964. Assay for friend leukemia virus: rapid quantitative method based on enumeration of macroscopic spleen foci in mice. Virology 24:513-518.

2. **Bailey, J. M., and N. Davidson.** 1976. Methylmercury as a reversible denaturing agent for agarose gel electrophoresis. Anal. Biochem. 70:75–85.
3. **Bender, W., and N. Davidson.** 1976. Mapping of poly(A) sequences in the electron microscope reveals unusual structures of type C oncornavirus RNA molecules. Cell 7:595–607.
4. **Dube, S. K., G. Gaedicke, N. Kluge, B. J. Weimann, H. Melderis, G. Steinheider, T. Crozier, H. Beckmann, and W. Ostertag.** 1973. Hemoglobin-synthesizing mouse and human erythroleukemic cell lines as model systems for the study of differentiation and control of gene expression, p. 99–135. *In* W. Nakahara, T. Ono, T. Sugimuna, and H. Sugano (ed.), Differentiation and control of malignancy of tumor cells. University of Tokyo Press, Tokyo.
5. **Dube, S. K., I. B. Pragnell, N. Kluge, G. Gaedicke, G. Steinheider, and W. Ostertag.** 1975. Induction of endogenous and of spleen focus-forming viruses during dimethylsulfoxide-induced differentiation of mouse erythroleukemia cells transformed by spleen focus-forming virus. Proc. Natl. Acad. Sci. U.S.A. 72:1863–1867.
6. **Friedrich, R., and G. Feix.** 1972. RNA-RNA hybridization in aqueous solutions containing formamide. Anal. Biochem. 50:467–471.
7. **Friend, C.** 1957. Cell-free transmission in adult swiss mice of a disease having the character of a leukemia. J. Exp. Med. 105:307–318.
8. **Kung, H. J., J. M. Bailey, N. Davidson, M. O. Nicolson, and R. M. McAllister.** 1975. Structure, subunit composition, and molecular weight of RD-144 RNA. J. Virol. 16:397–411.
9. **Kung, H. J., S. Hu, W. Bender, J. M. Bailey, N. Davidson, M. O. Nicolson, and R. M. McAllister.** 1976. RD-114, baboon, and woolly monkey viral RNAs compared in size and structure. Cell 7:609–620.
10. **Lilly, F., and T. Pincus.** 1973. Genetic control of murine viral leukemogenesis. Adv. Cancer Res. 17:231–277.
11. **Maisel, J., V. Klement, M. M-C. Lai, W. Ostertag, and P. Duesberg.** 1973. Ribonucleic acid components of murine sarcoma and leukemia viruses. Proc. Natl. Acad. Sci. U.S.A. 70:3536–3540.
12. **Ostertag, W., T. Cole, T. Crozier, G. Gaedicke, J. Kind, N. Kluge, J. C. Krieg, G. Roesler, G. Steinheider, B. J. Weimann, and S. K. Dube.** 1973. Viral involvement in the differentiation of erythroleukemic mouse and human cells, p. 493–520. *In* W. Nakahara, T. Ono, T. Sugimuna, and H. Sugano (ed.), Differentiation and control of malignancy of tumor cells. University of Tokyo Press, Tokyo.
13. **Ostertag, W., H. Melderis, G. Steinheider, N. Kluge, and S. K. Dube.** 1972. Synthesis of mouse haemoglobin and globin mRNA in leukaemic cell cultures. Nature (London) New Biol. 239:231–234.
14. **Ostertag, W., G. Roesler, C. J. Krieg, J. Kind, T. Cole, T. Crozier, G. Gaedicke, G. Steinheider, N. Kluge, and S. K. Dube.** 1974. Induction of endogenous virus and of thymidine kinase by bromodeoxyuridine in cell cultures transformed by friend virus. Proc. Natl. Acad. Sci. U.S.A. 71:4980–4985.
15. **Schildkraut, C., and S. Lifson.** 1965. Dependence of the melting temperature of DNA on salt concentration. Biopolymers 3:195–208.
16. **Steeves, R. A., R. J. Eckner, M. Bennett, E. A. Mirand, and P. J. Trudel.** 1971. Isolation and characterization of a lymphatic leukemia virus in the friend virus complex. J. Natl. Cancer Inst. U.S.A. 46:1209–1217.